



HAL
open science

Trajectory derived from the 3D linear wind field retrieved by a wind-profiler mesoscale network

Bernard Campistron, V. Puygrenier, B. Bénech, Fabienne Lohou, F. Saïd,
Clotilde Moppert, F. Cousin, E. Dupont

► **To cite this version:**

Bernard Campistron, V. Puygrenier, B. Bénech, Fabienne Lohou, F. Saïd, et al.. Trajectory derived from the 3D linear wind field retrieved by a wind-profiler mesoscale network. 16th Symposium on Boundary layer and Turbulence, Aug 2004, Portland, United States. hal-00141845

HAL Id: hal-00141845

<https://hal.science/hal-00141845>

Submitted on 15 Nov 2021

HAL is a multi-disciplinary open access archive for the deposit and dissemination of scientific research documents, whether they are published or not. The documents may come from teaching and research institutions in France or abroad, or from public or private research centers.

L'archive ouverte pluridisciplinaire **HAL**, est destinée au dépôt et à la diffusion de documents scientifiques de niveau recherche, publiés ou non, émanant des établissements d'enseignement et de recherche français ou étrangers, des laboratoires publics ou privés.



Distributed under a Creative Commons Attribution 4.0 International License

P 6.1 TRAJECTORY DERIVED FROM THE 3D LINEAR WIND FIELD RETRIEVED BY A WIND-PROFILER MESOSCALE NETWORK

Campistron^{1*} B., V. Puygrenier¹, B. Bénech¹, F. Lohou¹, F. Saïd¹,
C. Moppert¹, F. Cousin¹, and E. Dupont².

¹Laboratoire d'Aérodologie, UMR 5560 CNRS/UPS, Observatoire Midi-Pyrénées, Centre de Recherches Atmosphériques, 65300 Lannemezan, France.

² Electricité de France, Direction des Etudes et Recherches, 78401 Chatou, France.

1. INTRODUCTION

A key issue in the survey or analysis of pollution episodes lies in the documentation of the turbulent dispersion and transport of the pollutant in the atmospheric boundary layer (ABL). Usually these processes are investigated with numerical modeling. Actually with the rapid development of UHF wind profilers able to provide wind components, turbulent variables, mixing height with a fine time and vertical resolution in the ABL, we can expect in a very near future the set up of regional profiler networks devoted to real time pollution monitoring.

Toward this expectation we present and discuss a methodology, based on measurements made by a wind-profiler mesoscale network, which retrieves the 3D wind field (linear part) used to derive any type of air parcel trajectories. The technique is applied to observations collected during the ESCOMPTE campaign, devoted to pollution studies, which took place in France in the early summer 2001 in the Marseille region, along the Mediterranean coast. In situ aircraft measurements and constant volume balloon trajectories are used to compare and verify the performance of this based-radar methodology during sea and land breeze events. These cases studies, characterized by rapid temporal evolution and important spatial variations of the atmospheric fields, are particularly instructive in the analysis of the potentiality of the technique.

2. WIND-PROFILER NETWORK DATA

An overview of the scientific objectives of the ESCOMPTE program, the field campaign, and the instrumental facilities is given by Cros et al (2004). Figure 1 shows a limited area of the ESCOMPTE domain where a network of 4 UHF wind profilers were deployed during 4 weeks in June-July 2001. Alps foothills reaching 200 m in the north and east of the domain, ragged shoreline and the Berre pond in the central part make the topography of this coastal zone particularly complex. Extensive urbanization,



Figure 1. The UHF wind profiler network deployed during ESCOMPTE campaign. Sodar and VHF profilers locations are also shown.

strong density of industrial complexes, and the prevalent particular atmospheric conditions, make this region one of the most polluted in France.

The 4 UHF Doppler radars manufactured by Degreane (PCL1300) have the same technical characteristics: a 4 kW peak-power, a 1238 MHz transmitted frequency and a 150 m pulse width. Except for the profiler located at Aix-les-Milles, which made use of 3 beams only, the other ones worked with 5 beams: a vertical and four oblique ones disposed every 90° in azimuth with a 77° elevation angle. Operated in a continuous mode, they provided every 5 minutes in clear air and raining conditions vertical profiles of reflectivity, the three components of the wind, and the Doppler spectral width with a 75 m vertical step, from a height of 75 m AGL up to 2 to 3 km, depending on atmospheric conditions. The selection of the meteorological peak in the Doppler spectra is made with a 30-min-duration consensus technique mainly based on thresholds, vertical and temporal continuity. More details on the data processing, radar technique and signal scattering are found in Jacoby-Koaly et al (2002).

*Corresponding author address: Bernard Campistron, Centre de Recherches Atmosphériques, 65300 Lannemezan, France; e-mail: camb@aero.obs-mip.fr

3. METHODOLOGY

3.1 3D atmospheric fields

The method used here to derive the 3D (three dimensional) atmospheric fields from the UHF profilers network is described in Campistron (1997). The principle of the method, first developed for the French VHF radar regional network, is based on the assumption of the linearity of the meteorological fields inside a limited spatial and temporal domain. According to this hypothesis, a field of a quantity Φ measured by the profilers, function of the latitude θ , the longitude λ , the altitude z , and the time t , is represented by the following Taylor series limited to the linear terms:

$$\Phi(t_0+\Delta t, \theta_0+\Delta\theta, \lambda_0+\Delta\lambda, z_0+\Delta z) = \Phi(t_0, \theta_0, \lambda_0, z_0) + \Delta t \frac{\partial\Phi}{\partial t} + \Delta\theta \frac{\partial\Phi}{\partial\theta} + \Delta\lambda \frac{\partial\Phi}{\partial\lambda} + \Delta z \frac{\partial\Phi}{\partial z} + \xi. \quad (1)$$

where $(t_0, \theta_0, \lambda_0, z_0)$ is a reference point. ξ is the departure from the linear model. For a time t_0 and an altitude z_0 , the coefficients of the series, for each quantity measured by the profilers, are extracted through a weighted least-squares fitting making use of all the radar data $\Phi(t, \theta, \lambda, z)$ that verify:

$$t_0 - \Delta T/2 < t < t_0 + \Delta T/2 \quad \text{and} \quad z_0 - \Delta H/2 < z < z_0 + \Delta H/2.$$

The choice of the parameters ΔT and ΔH is crucial since it controls the filtering of the unresolved atmospheric scales and the attenuation of the data noise. For the data presented here, we use 150 m and 1 hour for the parameters ΔH and ΔT respectively. According to Campistron (1997) the resolved atmospheric scales are larger than about twice the mean horizontal dimension of the network, and therefore are greater here than about 60 km.

Equation (1) is solved in two steps; the first pass is used to remove data which are too distant from the linear model. Usually less than 5% of the data are removed. Only the remaining data are used in the linear fitting of the second pass. From the processing of the horizontal components of the wind, we can deduce, among other parameters, the horizontal divergence as a function of height and time. Vertical velocity is computed from the upward integration of the anelastic continuity equation with the assumption of a zero vertical velocity at ground level. Vertical profiles of $(\Phi_0, \partial\Phi/\partial t, \partial\Phi/\partial\theta, \partial\Phi/\partial\lambda, \partial\Phi/\partial z)$ function of time and height, are obtained when varying t_0 and z_0 . For the present study these vertical profiles were computed every 5 minutes and 75 m.

3.2 Trajectory

Let \mathbf{X}_0 and \mathbf{X}_1 the position vector of an air parcel at time t_0 and $t_1 = t_0 + \Delta t$, respectively. For sufficiently small time increment (here 5 min.), \mathbf{X}_1 is related to the

initial position \mathbf{X}_0 by the following first-order equation, also called "constant acceleration solution" (Stohl, 1998):

$$\mathbf{X}_1 = \mathbf{X}_0 + (d\mathbf{X}_0/dt + d^2\mathbf{X}_1/dt^2) \Delta t / 2 \quad (2)$$

The iterative application of Eq. (2) using air velocity components $d\mathbf{X}_i/dt$ provided by the profilers network determines completely the path of an air parcel identified by its starting position \mathbf{X}_0 . Forward or back trajectory is obtained depending on the positive or negative sign affected to Δt . Stohl (1998) offers an excellent and updated review on the computations and use of trajectories.

4. EXAMPLES OF RESULTS

The most important pollution episodes occur during anticyclonic situations that promote also in this coastal region land and sea breeze circulation. In this section, as an example of application of the above described methodology, the 2001 June 25 breeze event is presented.

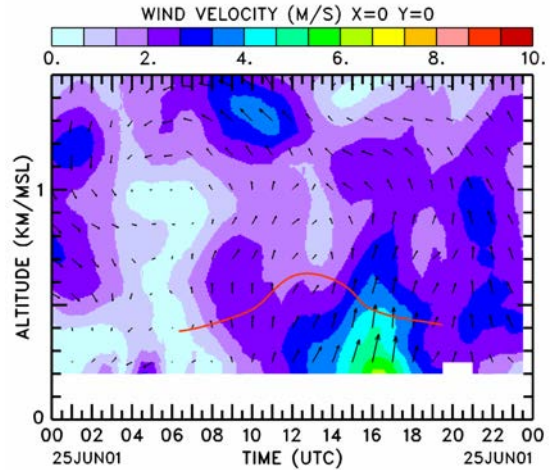


Figure 2. Time-height section of the wind vector restituted at the UHF profiler network centroid by the 3D radar methodology. The red curve represents the ABL top deduced from UHF reflectivity maximum.

Figure 2 shows a time-height section of the wind vector deduced by the 3D methodology at the network centroid (close to the site of the Marignane UHF). In spite of the temporal and vertical smoothing due to the technique, the fine features of the diurnal cycle of a breeze circulation is well reproduced: light ($\sim 1 \text{ ms}^{-1}$) northerly wind during the night (land breeze), and southerly wind (sea breeze) increasing regularly during the day to reach a maximum of 7 ms^{-1} in the middle of the afternoon at 1600 UTC.

In Fig. 2 the curve of the height of the ABL top as a function of time is plotted. It corresponds to the location of the UHF reflectivity maximum (Angevine et al, 1994). Because of the relative cool and humid marine air advection, one can see that coastal ABL is

usually shallow (Moppert et al, 2004), and for this case study ABL depth does not exceed 600 m MSL, whereas surface temperature reaches 25° C.

The horizontal wind circulation reconstructed thanks to the UHF network observations at a height of 400 m during land-breeze (0400 UTC) and sea-breeze (1300 UTC) is displayed in Fig. 3 (a) and (b) respectively.

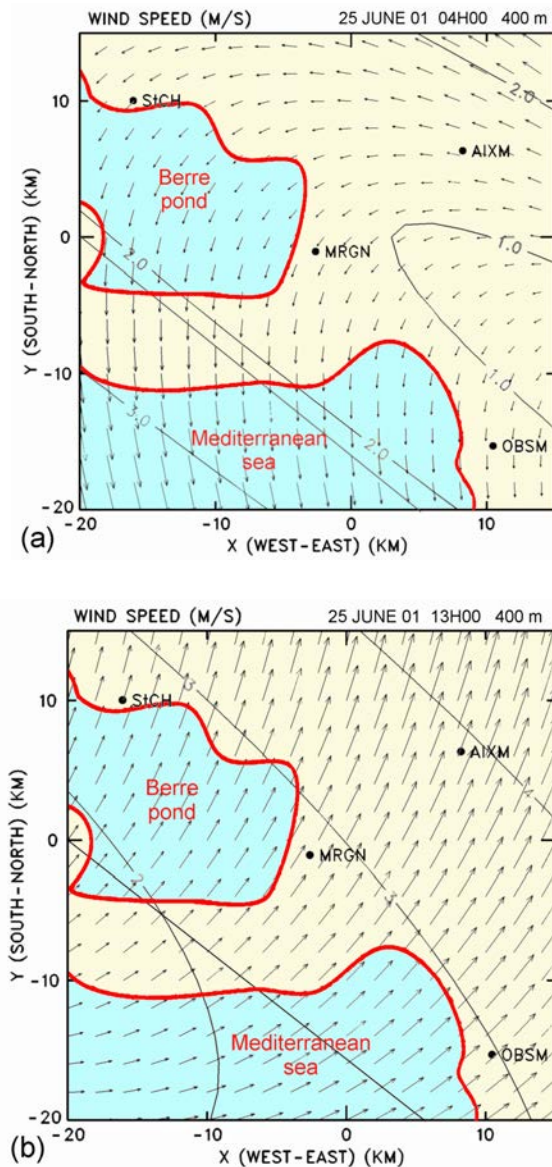


Figure 3. Horizontal plane at 400 m MSL of the wind field deduced from the observations of the UHF radars network (solid circles) at 0400 UTC (a) and 1300 UTC (b). Wind intensity contours (ms^{-1}) are superimposed.

Indeed the analytic linear field so deduced cannot be extended up to infinity. It is only valid in the network domain and in its close neighboring delimited by a radius which could be defined by the smallest resolved horizontal scale.

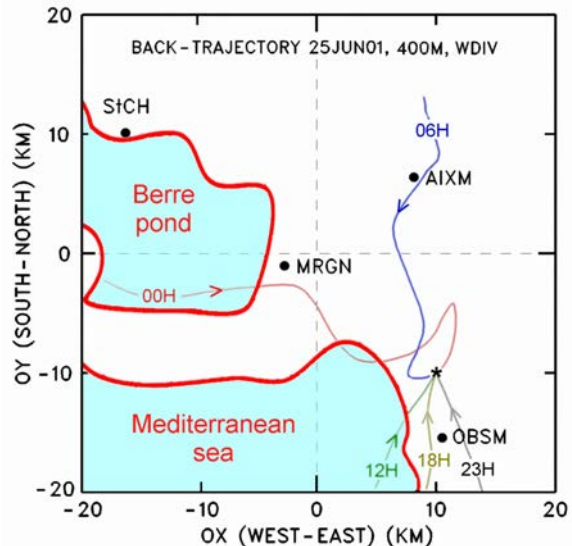


Figure 4. Back trajectories of air parcels arriving at different times on 25/06/01 above Marseille city (star) at a height of 400 m. The maximum duration of the plotted trajectories is 6 hours. Solid circles indicate UHF profiler locations.

An example of back trajectories of air parcels retrieved by the 3D methodology is shown in Fig. 4. The arriving point on 25/06/01 for several arriving hours is taken 400 m above Marseille city. The duration of the plotted trajectories is limited to 6 hours. The paths followed at different times by the air particle is well representative of the diurnal rotation of the wind direction during a breeze day. The most important source of chemical pollution is located at the south of the Berre pond. Figure 4 shows that for this day these pollutants reached Marseille around midnight.

5. PERFORMANCE EVALUATION

On 2001 June 26, at about 1150 UTC, the meteorological ARAT aircraft flew at an altitude of 750 m in the vicinity of the UHF network. The characteristics of this research aircraft can be found in Saïd et al (2004). Figure 5 (a) presents the ARAT path superimposed on the wind modulus contours deduced from the UHF network data.

Comparison of wind intensity and direction measured by aircraft and by the 3D profiler network along the ARAT trajectory is shown in Fig. 5 (b) and (c), respectively. Aircraft data were smoothed with a running mean applied over 3 km. The agreement is quite good. The 3D linear methodology was able to reconstitute the mesoscale trend observed on the in situ measurements. However it seems that there is a light offset in the network estimates lesser than $1 ms^{-1}$ and 20° . This can be attributed to the fact that the aircraft trajectory did not cross the network area but was displaced several km from it.

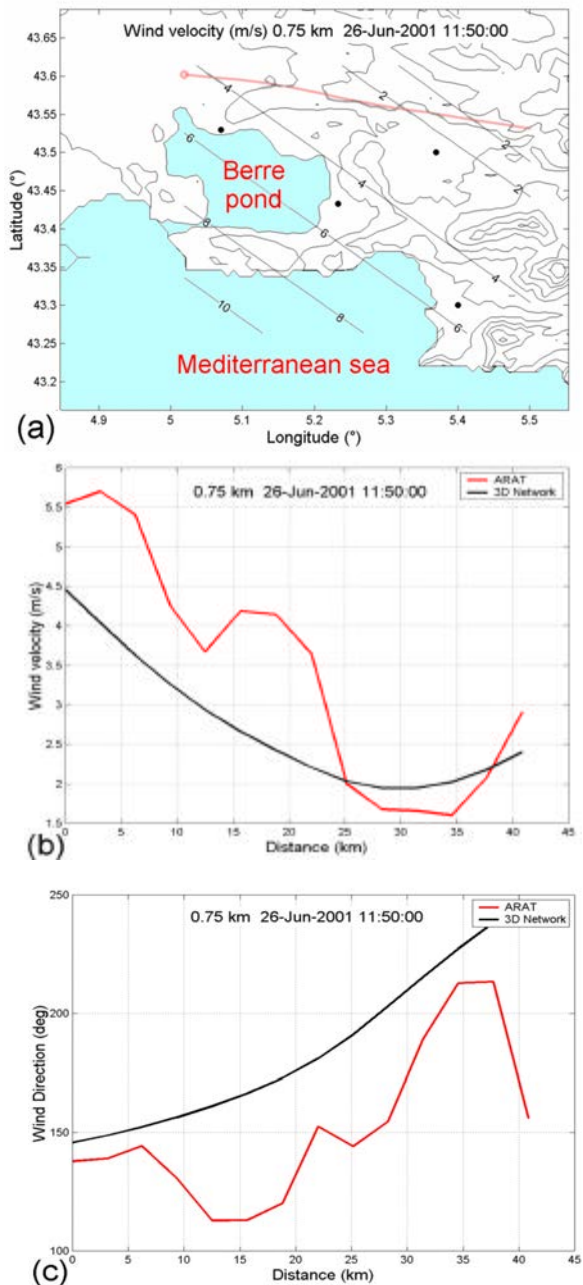


Figure 5. 2001 June 26, 1150 UTC, altitude 750M. Comparison between the wind derived from the UHF network and the wind measured by the ARAT aircraft. (a) ARAT path (red curve) and wind modulus contours (ms^{-1}) provided by the UHF network (solid circles). Comparison of the wind intensity (b) and direction (c) along the aircraft path.

During the campaign several constant volume balloons equipped for in situ measurements and GPS positioning were launched. They fly at constant density and so nearly at constant altitude. Roughly speaking, their trajectories are comparable to the ones followed by a Lagrangian particle moving with

the wind and with a null mean vertical velocity. These balloons often serve to assess trajectories deduced from numerical models. This application is also used here to test the accuracy of the trajectories deduced from the UHF profiler network. Two case studies are presented in the Figure 6 below. Note that Fig 6b corresponds to the day presented in Fig 5.

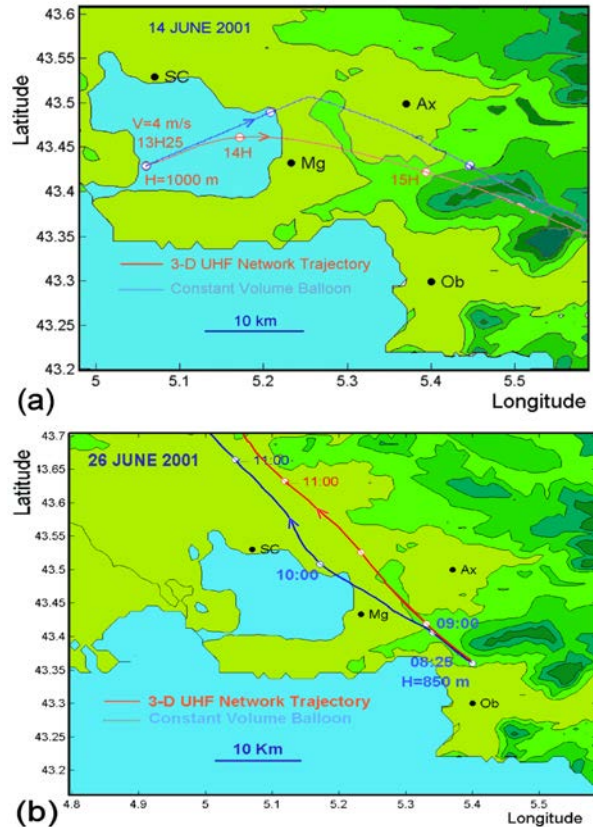


Figure 6. Trajectory of constant volume balloon (blue curve), and simulated air particle trajectory (red curve) at constant level starting at the same initial height and time than the balloon using wind horizontal velocity derived from the UHF network and null vertical velocity. Solid circles indicate the radar sites, and some hours of the trajectories passage are given. a) 2001 June 14; starting time 1325 UTC and constant level flight at 1000 m. b) 2001 June 26; starting time 0825 UTC and constant level flight at 850 m.

The detailed explanation of the balloon flights and 3D UHF network trajectories is given in the caption of Fig 6. For both days these two types of trajectories starting at two different points crossed the network domain. Their durations were about 2.5 hours and their lengths approximately 50 km. The constant level of the flight was in both cases just below or just above the ABL top and so in a zone of rapid vertical change of the wind.

On June 14 (Fig. 6a) there is an important temporal and spatial change of the wind which

induces a strong rotation on the balloon trajectory. This rotation is also observed in the UHF-network trajectory but it is not so acute and it occurs over a longer period of time. On June 26 (Fig. 6b), as the wind direction varied slowly in that part of the domain, both trajectories are nearly rectilinear and parallel. For these two cases studies the range departure between the trajectories is less than 5 km and so represents 10% of the total trajectories length.

6. CONCLUSION

More than a decade of UHF profilers operation has established the great interest of this remote sensing device in the investigation of atmospheric boundary layer. In the present paper we have presented a technique capable to retrieve the linear 3D atmospheric field from the observation collected by a mesoscale UHF profiler network. The 3D wind field is then used to reach the goal of this work which was to derive air parcel trajectories useful for pollution transport investigation.

In situ data collected during the experimental field ESCOMPTE demonstrated the good potentiality of the overall methodology in the case of breeze circulation. The assessment of the performance of the air trajectory and 3D wind field restitution will be continued on the basis of the numerous comparison cases with aircraft flights, constant balloon flights and mesoscale model runs (Meso-nh) made during ESCOMPTE.

Turbulence that prevails in the ABL tends to quickly remove the identity of air parcels which is the basic assumption for the trajectory construction. In order to take into account this phenomenon (i.e. the statistical nature of the atmospheric motion) it is necessary to introduce in Eq. 2 a turbulent velocity (Stohl, 1998). Information on the turbulent field can be extracted from UHF profilers data (Jacoby-Koaly, 2002). This necessary improvement of the method will provide, instead of a single air path, a trajectory plume more appropriate for the investigation of pollutant transport and dispersion in the ABL.

7. ACKNOWLEDGMENTS

This research was mainly supported by CNRS, INSU/PATOM, Météo-France and EDF. We gratefully acknowledge all the laboratories and working groups which made possible the carrying out of the ESCOMPTE campaign.

8. REFERENCES

Angevine, W. M., White, A. B., and Avery, S. K.: 1994, 'Boundary-Layer Depth and Entrainment Zone Characterization with a Boundary-Layer Profiler', *Boundary-Layer Meteorol.*, **68**, 375-385.

Campistron, B., 1997: Retrieval of the 3D kinematic from a regional network of wind profilers, *28th Conference on Radar Meteorology*, 83-84.

Cros, B., P. Durand, H. Cachier, P. Drobinski, E. Fréjafon, C. Kottmeier, P. E. Perros, V.-H. Peuch, J. L. Ponche, D. Robin, F. Saïd, G. Toupance, and H. Wortham, 2004: The ESCOMPTE program: an overview. *Atmos. Res.*, **69**, 241-279.

Jacoby-Koaly S., B. Campistron, S. Bernard, B. Bénech, F. Girard, J. Dessens, E. Dupont, and B. Carissimo, 2002: Turbulent dissipation rate in the boundary layer via UHF wind profiler Doppler spectral width measurement. *Boundary-layer Meteorology*, **103**, 361-389.

Moppert, C, F. Saïd, A. Brut, V. Puygrenier, B. Campistron, B. Bénech, F. Lohou, and F. Cousin, 2004: Stratification of the lower troposphere during the ESCOMPTE campaign. *16th Symposium on Boundary Layer and Turbulence*, Portland USA, this issue.

Saïd, F., U. Corsmeier, N. Kahlhoff, C. Kottmeier, M. Lothon, A. Wieser, T. Hofherr, and P. Perros, 2004: ESCOMPTE experiment : intercomparison of four aircraft dynamical, thermodynamical, radiative and chemical measurements. *Atmos. Res.*, in press.

Stohl, A., 1998: Computation, accuracy and applications of trajectories – A review and bibliography. *Atmos. Env.*, **32**, 947-966.